Pergamon

PII: S0042-6989(97)00155-7

Vision Res., Vol. 38, No. 1, pp. 61–70, 1998
© 1997 Elsevier Science Ltd. All rights reserved
Printed in Great Britain
0042-6989/98 $19.00 + 0.00

Peripheral and Central Factors Limiting the Development of Contrast Sensitivity in Macaque Monkeys

LYNNE KIORPES,*‡ J. ANTHONY MOVSHON†

Received 17 February 1997; in revised form 7 May 1997

The aim of this study was to evaluate the contribution of peripheral and central factors to the development of visual sensitivity. We used the approach of (Pelli, 1981, 1990) to evaluate the hypothesis that intrinsic noise is high in infants compared with adults, and therefore sets an important limit on contrast sensitivity in infants. We measured contrast thresholds in the presence of various levels of dynamic spatiotemporal broadband noise in infant monkeys, and evaluated the developmental changes in contrast threshold and intrinsic noise. Our data show that intrinsic noise is high in infants and falls with contrast threshold during development. However, contrast thresholds in high-contrast noise also fall during development, although by a smaller amount. Therefore, while changes in intrinsic noise set an important limit on the development of contrast sensitivity across spatial frequencies, changes in non-additive sources of noise also contribute, particularly at high spatial frequencies. We interpret these results in terms of Pelli's hypothesis about the sources of additive and non-additive noise affecting visual detection. In these terms, additive noise reflects peripheral factors and non-additive noise reflects central ones. Our results suggest that changes in peripheral sources of noise represent an important limit for the development of visual sensitivity. © 1997 Elsevier Science Ltd

Contrast sensitivity Intrinsic noise Visual development Monkey

INTRODUCTION

Contrast sensitivity and spatial resolution are immature in newborn primates. These visual functions improve approximately 10-fold over the first year after birth in macaque monkeys (Boothe, Kiorpes, Williams, & Teller, 1988; Kiorpes, 1992). Recently, there has been increased interest in understanding the factors that limit visual sensitivity in newborn infants and determine the subsequent developmental time course. While there are changes in the optics of the eye that will lead to small improvements in performance, it is generally agreed that changes in the nervous system are of far greater importance. Very marked changes in photoreceptor outer segment morphology have been detailed by Yuodelis & Hendrickson (1986). Calculations based on these changes suggest that infant photoreceptors are substantially less efficient at capturing light than adult ones. Banks & Bennett (1988), Brown, Dobson, & Maier (1987), Brown (1993), and Wilson (1988) have recently evaluated these and other factors limiting infant visual development. These studies concluded that while one would expect an overall improvement in quantum efficiency during development in the infants, this expected improvement is not sufficient to fully account for the extent of the change in infant contrast sensitivity; changes in the signalling properties of the neurons carrying photoreceptor signals through the nervous system must also be involved. It is therefore desirable to try to learn the degree to which changes in peripheral and central mechanisms limit visual performance during development.

Psychophysical approaches based on noise masking measurements may help us understand the limitations on sensitivity by dividing them into peripheral (early visual pathways) and central factors. This idea was proposed by Barlow (1977) to characterize the efficiency of the human visual system, and was elaborated by (Pelli, 1981, 1990), Burgess, Wagner, Jennings, & Barlow (1981), and Kersten (1984), among others. The scheme proposed by Pelli (1990), under certain assumptions, attributes overall visual efficiency to the combined action of two stages, one presumed to correspond to the input stage of visual processing and the other to elements later in the visual

*Center for Neural Science, New York University, New York, NY 10003, U.S.A.

†Howard Hughes Medical Institute, New York University, New York, NY 10003, U.S.A.

‡To whom all correspondence should be addressed at Center for Neural Science, New York University, 4 Washington Place, Room 809, New York, NY 10003-1056, U.S.A. [*Tel*: (212) 998 7897; *Fax*: (212) 995 4183; *Email*: lynne@cns.nyu.edu].

system. Pelli based his arguments on the well-known additive form of results from contrast detection experiments performed in masking noise, in which squared contrast thresholds rise in direct proportion to the squared contrast of added noise, plus a constant. From this constant, Pelli deduced the amount of additive intrinsic noise that affects contrast detection, expressed in units equivalent to the added noise. We have followed this scheme and similarly use "equivalent noise" to estimate the level of early "intrinsic" noise in the visual pathway. By measuring intrinsic noise and comparing its magnitude with visual sensitivity in young monkeys of different ages, we hoped to evaluate the hypothesis that infant contrast threshold is high as a result of high levels of intrinsic noise. The extent to which contrast thresholds and intrinsic noise fall together during development may establish the contribution of peripheral factors to sensitivity in young animals. In addition to intrinsic noise estimated in this way, there must also be non-additive "central" factors that affect thresholds; Pelli's analysis derives these from thresholds measured at high noise levels. To the degree that these thresholds fall during development, central, non-additive factors may present the most important limit.

We measured contrast thresholds in dynamic visual noise in infant monkeys, and evaluated the developmental changes in contrast threshold and intrinsic noise. Our data show that intrinsic noise is high in infants and falls during development, suggesting that peripheral factors are an important limit on the development of visual sensitivity. Contrast thresholds measured in high levels of noise fall as well, however, so we conclude that central changes must also be involved. Some of these results have been presented previously (Handel, Kiorpes, & Movshon, 1993; Kiorpes, Skoczenski, & Movshon, 1995).

METHODS

Subjects

Thirteen young *Macaca nemestrina* monkeys were subjects in this study. All animals were born at the Washington Regional Primate Research Center, and were hand-reared in the Visual Neuroscience Laboratory at New York University. All animal care conformed to guidelines approved by the New York University IACUC and the NIH Guide for Care and Use of Laboratory Animals. The animals ranged in age from 1 to 18 months at the time of testing. Their visual environment was a normal laboratory environment, which was enriched with a wide variety of appropriate visual and tactile stimuli. The animals were also given daily opportunities for interaction with other monkeys and humans.

Stimuli

Stimuli were presented on a Nanao T660i monitor with a mean luminance of 56 cd/m^2. The display subtended 36 deg at 60 cm, the viewing distance used for young infants. Typically, animals older than 1 year were tested at distances of 100–120 cm. Stimulus presentation was controlled by a computer via an ATVista graphics board (Truevision). We used patches of sinusoidal grating vignetted by a 2D spatial Gaussian, whose contrast was ramped on over 200 msec. Grating spatial frequency ranged from 0.5–4.2 cyc/deg. The standard deviation of the spatial Gaussian was 3 deg. Once the grating reached full contrast (after the 200 msec ramp which was accompanied by a tone), the animal was free to respond. Since the animals were freely viewing, the viewing duration was not controlled precisely. However, response latencies, when measured, were typically about 500 msec. We did not notice a tendency for younger animals to view the display for different durations than older animals did; in any case, variations in viewing duration around 500 msec have little effect on sensitivity and would not be likely to have a significant effect on the results. The grating patches were presented alone and in the presence of random spatiotemporal broadband noise. The noise was refreshed with a new random noise field at a rate of 53 Hz and was interleaved on alternate frames with the grating. The noise was continuously present and filled the entire display. Noise pixel size was 11.6 min (at 60 cm); there were 188×144 noise pixels across the screen. Noise Michelson contrast ranged from 0.01–0.50. In some early experiments we used noise in which the luminance distribution of pixel values was uniform, but for most experiments we used binary noise (i.e., noise whose pixels took on one of two values), because binary noise provides the greatest contrast energy at a given physical contrast. The details of the algorithm used for noise generation can be found in Gegenfurtner & Kiper (1992).

Behavioral methods

On each trial, a grating patch was presented on either the left or right side of the video display, 10 deg from center. The monkey's task was a spatial two-alternative forced-choice; she indicated on which side of the display the grating patch had appeared. For very young infants (generally those younger than 12 weeks), we used a procedure that we call "reinforced preferential looking". The procedure combines preferential looking and operant techniques. The animals were placed in a cage with a facemask mounted on one wall (Williams, Boothe, Kiorpes, & Teller, 1981). Their looking behavior was monitored via a video camera directed at the eyehole of the facemask. During training, the infant monkeys were rewarded for directing their gaze toward a 2×2 deg square of flickering, random noise located in the center of an otherwise blank display. A human observer watched the animal's looking behavior on a video monitor connected to the camera. When the animal oriented toward the center of the display, a grating patch was presented to the left or right of center. The animal indicated the side on which the grating had appeared with a leftward or rightward directed eye movement. The human observer, who was blind as to the side of stimulus presentation, made a response on the computer keyboard

to indicate the direction of the monkey's eye movement. The monkey was rewarded with a squirt of infant formula or apple juice for the observer's correct responses. Once the animal was trained to reliably detect and indicate the side of stimulus presentation, she was allowed to freely view the display. The flickering square was replaced with a small cross that could be used to re-orient the animal to center if necessary. We saw no sign that the animals used peripheral vision to detect the stimulus; the infants typically scanned the display looking for the stimulus, then maintained their gaze on one side or the other to indicate their response. Older animals were trained to pull one of a pair of grab bars located on the front of the cage to indicate the side of stimulus presentation. They freely viewed the display and were rewarded for correct bar pulls; errors were signalled by a tone. Further details of these procedures may be found in earlier reports (Kiorpes, Kiper, & Movshon, 1993; Kiorpes & Kiper, 1996).

Contrast threshold for each stimulus condition was established using the method of constant stimuli. Each threshold was based on at least 200 trials; we collected 50–100 trials at each of 3–5 contrast levels chosen to span the performance range from 50–100% correct. Contrast threshold for each spatial frequency was measured in the absence of noise and either in the presence of each of a series of noise masks, or in some cases in a mask of the highest noise contrast (0.50). Data collection was counterbalanced across noise contrast level. Threshold estimates and standard errors were calculated using Probit analysis (Finney, 1971) of the log-transformed data sets.

RESULTS

It is generally accepted that grating detection is mediated by mechanisms that are selective for both spatial and temporal frequency. For this reason, the contrast of the noise is not the appropriate measure of its strength; that is best given in units of spectral density, or contrast power per unit bandwidth, which is the expected contrast power of a sample of the noise in a unit interval of spatiotemporal frequency. We calculated the spectral density of the noise for each set of spatiotemporal characteristics used. Within any given set of conditions, there is, of course, a consistent relationship between noise spectral density and noise contrast. That relationship, for the binary noise conditions used throughout most of this study, is shown by comparing the upper and lower abscissas in Fig. 1. The upper abscissa shows the spectral density of the noise; the lower abscissa shows the corresponding noise contrast.

Figure 1 illustrates the variation in contrast threshold with the strength of the masking noise; the isolated points on the left side of the plot indicate the measured contrast threshold for each stimulus in the absence of noise (unmasked contrast threshold). As expected (Pelli, 1990), at low levels of added stimulus noise, thresholds were little affected and the function was flat. This is the range over which intrinsic noise exceeds stimulus noise. At high noise levels, thresholds rise in proportion to noise contrast and the function has a slope of 1. This behavior is well known and is described by the relationship:

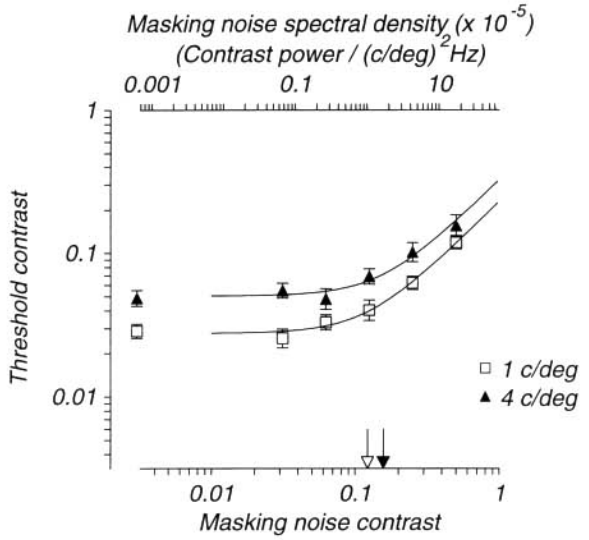

FIGURE 1. Representative masking functions for a 16-week-old monkey at two spatial frequencies, 1 and 4 c/deg (squares and triangles, respectively). The variation in contrast threshold is plotted as a function of masking noise contrast; noise spectral density is shown on the upper abscissa. The isolated data points are the measured unmasked thresholds for each spatial frequency. The open and filled arrows point to equivalent noise contrast (N_{eqC}) for the 1 and 4 c/deg data sets, respectively.

$$C = R_{sn}\sqrt{N^2 + N_{eq}^2} \quad (1)$$

where C is contrast threshold, N is the contrast power of the masking noise, R_{sn} is a constant giving the observer's overall signal-to-noise ratio, and N_{eq} is the "equivalent" intrinsic noise, referenced back to the visual scene in units equivalent to the masking noise power. When $N = N_{eq}$, contrast threshold is elevated by $\sqrt{2}$; this point is indicated on the abscissa with arrows for each curve. For the remainder of the paper, we will give noise strength in units related to the contrast of our "standard" noise (binary noise of our standard pixel size and frame rate), rather than the spectral density of the noise, since these units are more intuitive for most readers. For values given in contrast units we will use the terms N_C and N_{eqC} in place of N and N_{eq}. The constant R_{sn} gives the system's overall signal to noise ratio at threshold, expressing the threshold contrast as a proportion of the summed intrinsic and masking noises. Intuitively, R_{sn} determines the vertical position of the masking function, while N_{eq} determines its horizontal position.

As noted, throughout most of the study we used dynamic noise with a binary amplitude distribution. In some early cases, we used dynamic noise with a uniform amplitude distribution. Since the root mean square contrast of the amplitude distribution of the noise, presumably its masking strength, is given by the standard deviation of the amplitude distribution, and since uniform noise has lower standard deviation than binary noise, we compared equivalent noise contrast measured using

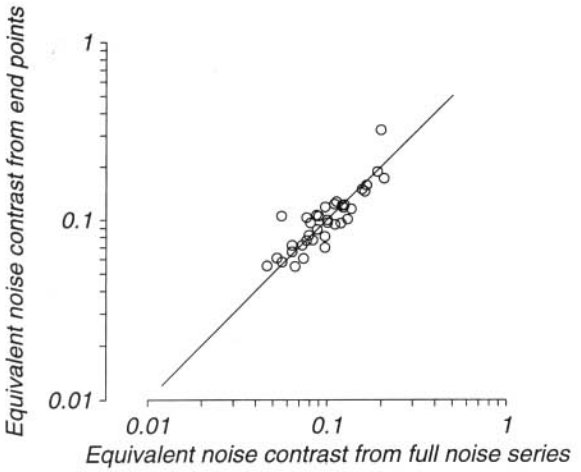

FIGURE 2. N_{eqC} estimated from the full range of masking contrasts is plotted against that estimated from only the unmasked threshold and the highest noise contrast from each data set. The data are from nine animals tested at various ages and spatial frequencies. The data cluster around the diagonal, which indicates slope of 1, showing good correspondence for equivalent noise contrast estimated by the two procedures.

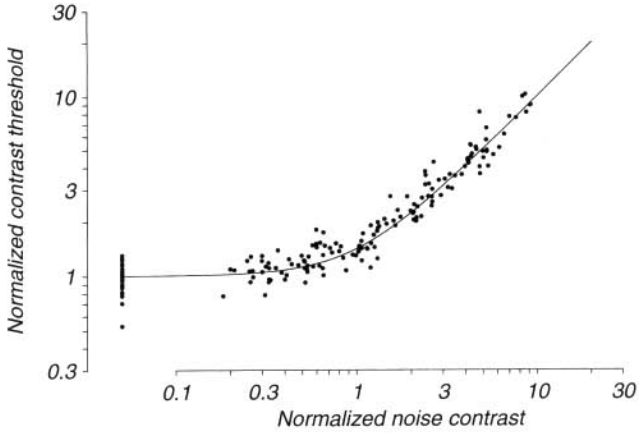

FIGURE 3. Masking data from 10 monkeys, collapsed across spatial frequency and age, are normalized on both threshold and N_{eqC} (see text for details). Comparison of the data with the curve shows that there is no systematic deviation.

uniform and binary noise distributions in three animals as a control. We calculated N_{eq} for each data set using the spectral density of the noise distribution and then scaled the values to be equivalent in contrast for our standard noise. Our estimated N_{eqC} was similar for the different noise conditions, so we included data collected using uniform noise in the population data. As stated above, in most cases we measured contrast threshold at each of a series of noise contrast levels, as well as in the absence of noise, as illustrated in Fig. 1. In some cases, we measured contrast threshold only in the absence of noise and in the presence of the highest noise contrast (0.50), to obtain a rapid estimate of equivalent noise contrast. Figure 2 illustrates the reliability of estimates of equivalent noise contrast based on only the end points of the series as opposed to the full series. These data are from nine animals tested at several ages and spatial frequencies. It is clear that the estimates of equivalent noise contrast are very similar, whether based on only the no-noise and highest noise points or based on the full series. Thus, we included estimates of equivalent noise contrast based only on two points in cases where there were no full series data at a given age; this was the case for most of the data presented for 2.1 c/deg.

To be sure that the theory and assumptions behind the noise masking paradigm were applicable to the monkey it was important to verify that the behavioral data conformed to the expected function. While this is apparent from individual data sets such as those shown in Fig. 1, it is important to establish whether the data as a whole showed any systematic variation from the expected function. Figure 3 shows that there was not. The data points are from multiple data sets collected from 10 monkeys at various ages. Each data set was fit by equation (1), and the data were then shifted horizontally and vertically on these log–log axes to make the fitted values of unmasked threshold and N_{eqC} equal 1. The data are consistently and uniformly close to the standard curve, showing that equation (1) provided a good description of the data.

While all of our data fit the template well, the robustness of our estimate of intrinsic noise depended on the degree of masking observed. We numerically simulated the accuracy with which N_{eq} was determined by the data. When N_{eq} is less than 25–50% of the maximum available noise contrast, it is estimated with roughly $\sqrt{2}$ less reliability than the contrast threshold. When N_{eq} approaches the maximum noise contrast, the reliability becomes appreciably worse. In cases where we did not have sufficient noise contrast to mask threshold, for example, some very young infants viewing high spatial frequency stimuli, we did not attempt to estimate N_{eq}. The results of these numerical simulations are reflected in our calculations of slopes involving N_{eq} (see below).

Developmental data for two monkeys are shown in Fig. 4. Each panel is similar in format to Fig. 1. The open symbols in each case represent data at one young age and filled symbols represent data collected at one older age from the same animal under the same test conditions. Masking functions are shown for each animal at two spatial frequencies: 1 (upper panels) and 4 c/deg (lower panels). The arrows point to equivalent noise contrast (N_{eqC}) for each function. At the lower spatial frequency for these animals, 1 c/deg, there was little change in unmasked contrast threshold between the test ages (isolated points to the left of the curves) and there was little difference in equivalent noise contrast for the data sets (compare open and filled arrows). At the higher spatial frequency, there was a substantial decrease in unmasked contrast threshold between the younger and older test ages for both monkeys, and there was an obvious concurrent change in equivalent noise contrast. This result suggests that intrinsic noise, as estimated by equivalent noise contrast, changes during development as

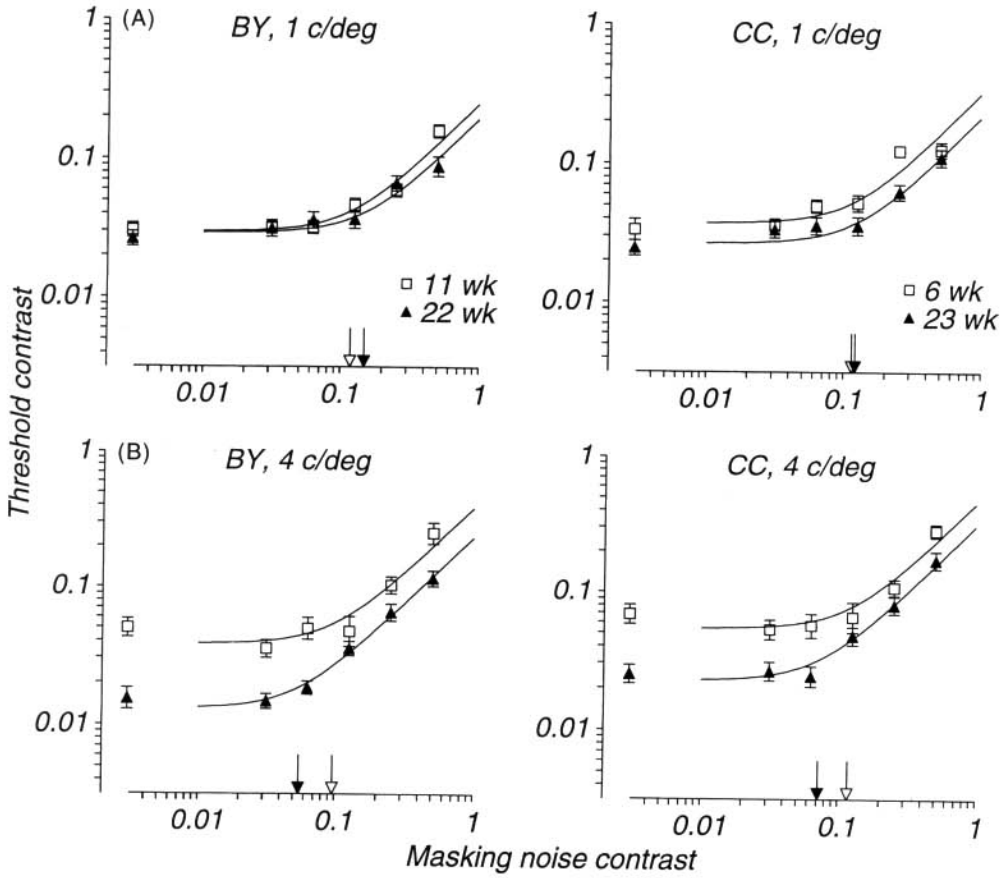

FIGURE 4. Contrast threshold is plotted as a function of noise contrast for two monkeys at two spatial frequencies and two ages. The top panels show data for the low frequency, 1 c/deg, and the bottom panels show data for the high frequency, 4 c/deg. Each panel shows data collected at one young (open squares) and one older (filled triangles) age. The open and filled arrows point to N_{eqC} for the young and old data sets, respectively. Symbols and axes are the same as in Fig. 1.

does contrast threshold. However, it is important to note that the change in unmasked contrast threshold is not proportional to the change in equivalent noise contrast. If it were, each pair of curves would come together at high noise contrasts. Instead, the functions rise in parallel with one another but do not meet.

As many previous experiments have shown, contrast threshold decreases during development. The change in unmasked contrast threshold with age for the population of monkeys in this study is shown in Fig. 5 for all spatial frequencies tested. The data for each spatial frequency are plotted against a separate ordinate for clarity, with the lowest frequency at the top and the highest at the bottom. As expected, contrast threshold decreased linearly with log age. The overall extent of the improvement in threshold was about 1 log unit for the low spatial frequencies, but was greater for the highest frequency. We performed a regression analysis to compare the change in threshold with age across spatial frequencies. This analysis showed that the slopes of the functions relating log contrast threshold and log age were close to −1 for 0.55 and 4.2 c/deg, but were somewhat lower for 1.0 and 2.1 c/deg. Table 1 presents regression slopes and correlation coefficients (in parentheses) for each comparison.

We next evaluated the change in equivalent noise contrast with age. Figure 6 shows the change in N_{eqC} with age for the same population as Fig. 5. There was a more gradual change in equivalent noise contrast than in unmasked threshold with log age for all spatial frequencies. The regression analysis showed that the slopes of the functions relating log equivalent noise contrast and log age were lower overall compared with the change in threshold; they were close to −0.3 for all spatial frequencies except 0.55 c/deg (see Table 1).

These comparisons suggest, as did the individual data

TABLE 1. Slopes (and correlation coefficients) of various functional relationships as a function of spatial frequency (* denotes a non-significant correlation)

Spatial frequency (c/deg)	0.55	1.0	2.1	4.2
Age/threshold	−0.91 (0.87)	−0.63 (0.81)	−0.65 (0.74)	−0.97 (0.87)
Age/N_{eqC}	−0.76 (0.75)	−0.28 (0.46)	−0.38 (0.53)	−0.39 (0.57)
Threshold/N_{eqC}	1.15 (0.77)	1.54 (0.71)	1.37 (0.81)	1.91 (0.79)
Age/R_{sn}	−0.18 (0.27)*	−0.35 (0.64)	−0.28 (0.53)	−0.57 (0.81)
Threshold/R_{sn}	3.66 (0.38)*	1.99 (0.62)	2.55 (0.59)	1.83 (0.80)

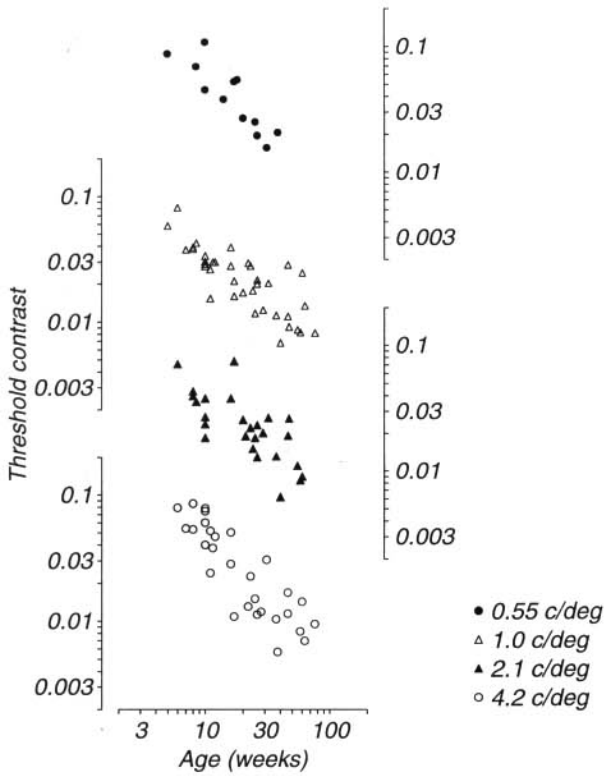

FIGURE 5. Threshold contrast is plotted as a function of age in weeks for each spatial frequency tested. Each data set is plotted against the adjacent ordinate; the lowest frequency tested is plotted at the top and the highest is plotted at the bottom. The data are all aligned vertically on the age axis. The data for each spatial frequency include data from all animals tested at that frequency.

in Fig. 4, that both contrast threshold and intrinsic noise decrease during development, but not to the same extent. To evaluate the relationship between these measures, we plotted unmasked contrast threshold against equivalent noise in Fig. 7. The variation in contrast threshold with N_{eqC} is shown for each spatial frequency, for all monkeys and ages, in the same format as Fig. 5. Clearly there was a strong correlation between unmasked contrast threshold and N_{eqC} for all spatial frequencies. However, for all except for the lowest spatial frequency, the relationships appear to have a slope greater than 1 (dashed lines). A slope of 1 would be expected if changes in threshold were wholly due to changes in intrinsic noise. Table 1 includes slope estimates for these data sets, calculated taking into consideration estimation errors in both threshold and equivalent noise contrast (see Press, Teukolsky, Vetterling, & Flannery, 1992). Indeed, for all frequencies except 0.55 c/deg, these slopes are substantially greater than 1.

Thus, it seems that changes in intrinsic noise, as measured by equivalent noise contrast, account for some, but not all, of the variation in contrast threshold during development. The remaining variance may be captured by changes in threshold in the presence of high masking noise contrast, i.e., the signal to noise ratio measured by the constant R_{sn} in equation (1). As noted earlier, the upper portion of the masking functions typically did not converge as the functions shifted with age (refer to Fig. 4). This suggests that there was also a change in contrast threshold in high noise with age. Figure 8 shows the

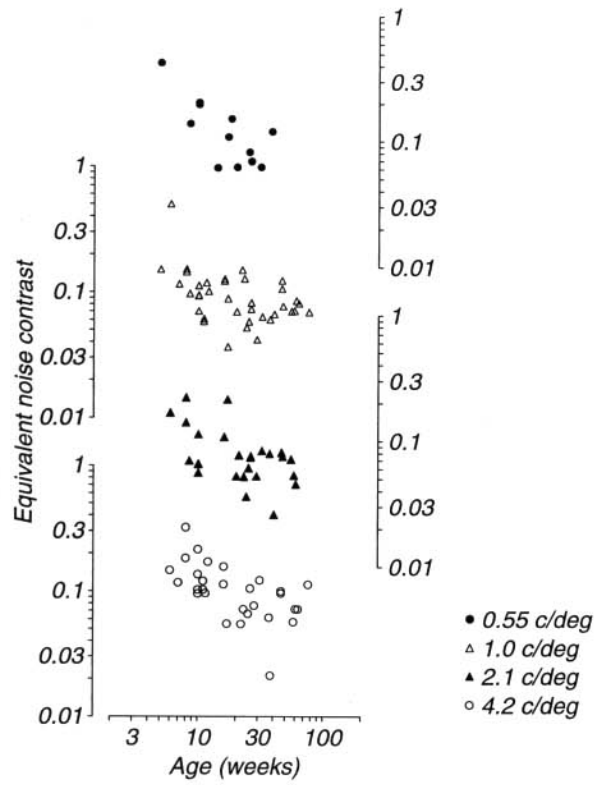

FIGURE 6. Equivalent noise contrast (N_{eqC}) is plotted as a function of age. Axes and symbols are the same as in Fig. 5.

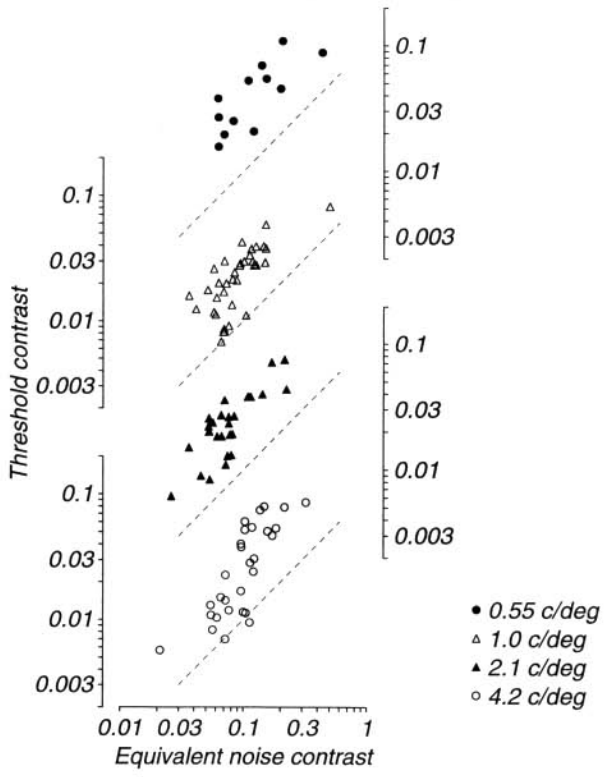

FIGURE 7. Threshold contrast is plotted as a function of equivalent noise contrast. The dashed lines under each data set represent a slope of 1. Axes and symbols are otherwise the same as in Fig. 5.

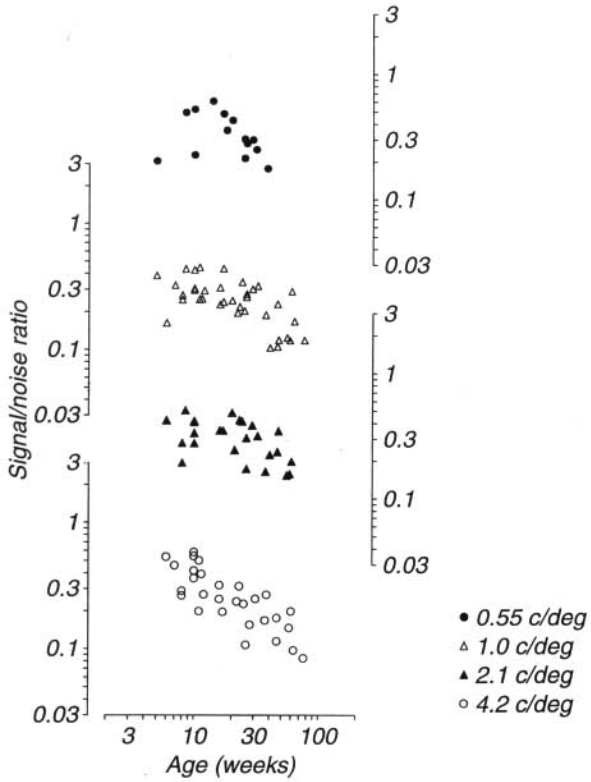

FIGURE 8. Signal to noise ratio (R_{sn}) is plotted as a function of age. The format is the same as in Fig. 5.

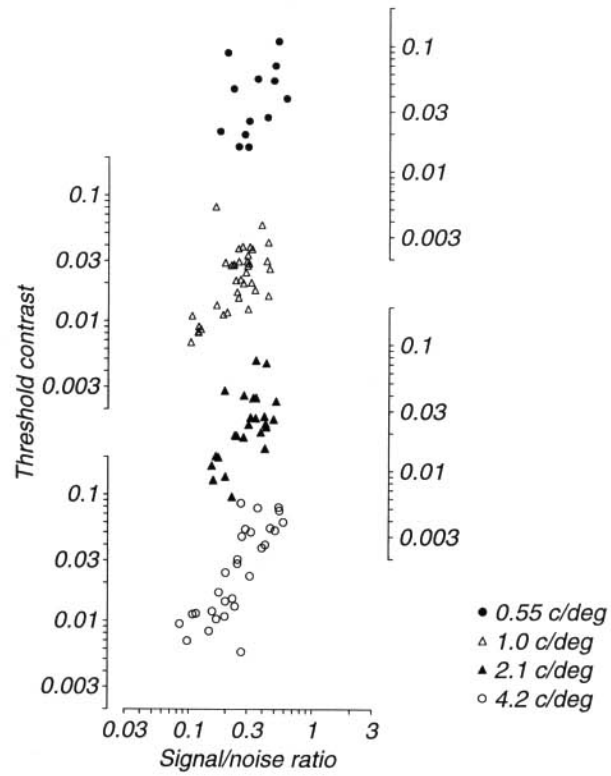

FIGURE 9. Threshold contrast is plotted as a function of R_{sn}. The format is the same as in Fig. 5.

variation in signal-to-noise ratio (R_{sn}) as a function of age for each spatial frequency. At the low spatial frequencies these data appear quite flat, suggesting that there was only a slight variation in signal-to-noise ratio with age. But this was not the case at 4.2 c/deg. There was a substantial change in signal-to-noise ratio with age at this higher frequency; in fact, this was quantitatively more important than the change in equivalent noise contrast (see Table 1). To examine the relationship between signal-to-noise ratio and unmasked contrast threshold for each spatial frequency, we plot threshold as a function of R_{sn} in Fig. 9. Because there was little variation in R_{sn} for the lower spatial frequencies, the slopes for these data sets were quite steep (see Table 1) indicating little covariation. At 0.55 c/deg there was in fact no significant correlation between signal-to-noise ratio and either unmasked threshold or age. On the other hand, there was greater variation in R_{sn} at 4.2 c/deg, and the relationship between signal to noise ratio and unmasked threshold is clear. Again, Table 1 includes slope estimates for these data sets, calculated taking into consideration estimation errors in both threshold and signal-to-noise.

DISCUSSION

Our aim was to deduce from psychophysical measurements the extent to which peripheral and central factors limit the development of spatial contrast sensitivity. Our results show that intrinsic noise is high in young infants and falls with contrast threshold during development. This result is consistent with the conclusions of Brown (1994), who estimated intrinsic noise in human infants using a luminance discrimination paradigm. That intrinsic noise is higher in infants than adults suggests that there are important peripheral limits on contrast sensitivity in young infants. However, our data also show that thresholds at high noise levels fall during development, particularly at 4.2 c/deg, the highest spatial frequency we tested. This result is summarized in Fig. 10, and supports the notion that central factors must also contribute to contrast sensitivity development.

It is important to consider first what is measured by changes in N_{eqC} and R_{sn} ("intrinsic noise" and "signal to noise ratio"). Formally, equation (1) describes masking functions in terms of an additive and a multiplicative constant (N_{eqC} and R_{sn}, respectively). We have followed Pelli's (1990) logic in attributing N_{eqC} to peripheral factors and R_{sn} to central ones, but it should be clear that this distinction may not be absolute. There is good reason to believe that noise in the peripheral elements of the visual pathway is approximately additive (e.g., Baylor, Lamb, & Yau, 1979; Croner, Purpura, & Kaplan, 1993; Troy & Lee, 1994), and it is also clear that non-additive factors contribute extensively to the variability measured in neurons in the central visual pathways (e.g., Tolhurst, Movshon, & Thompson, 1981, Tolhurst, Movshon, & Dean, 1983; Vogels, Spileers, & Orban, 1989; Britten, Shadlen, Newsome, & Movshon, 1993; Shadlen & Newsome, 1994). It is, however, going beyond the

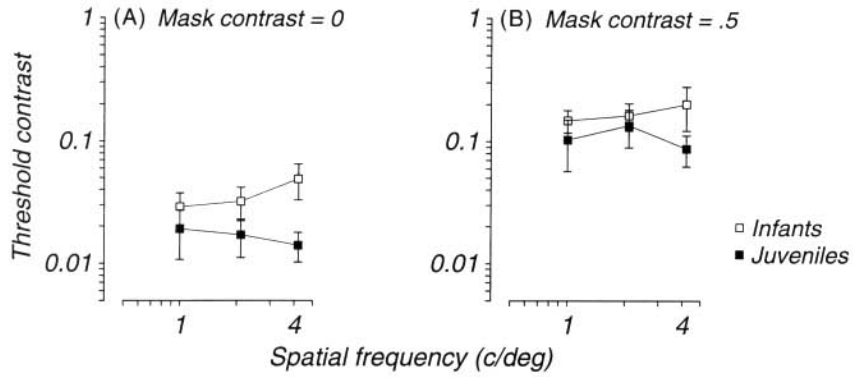

FIGURE 10. Threshold contrast is plotted for no noise mask (A) and high noise mask (B) conditions from animals for which longitudinal data were available. We show data for three spatial frequencies: 1, 2.1, and 4.2 c/deg, from seven monkeys. The criteria for inclusion were (1) we had thresholds for at least two of the three spatial frequencies; (2) within each of two age ranges: 12 weeks or younger (infants; open squares; range 7–12 wks) and 20 weeks or older (juveniles; filled squares; range 22–60 weeks). Five monkeys had complete data sets at all three spatial frequencies; two had complete data at two spatial frequencies. The data points are mean thresholds and standard deviations for $n = 6$ (2.1 and 4.2 c/deg) or $n = 7$ (1.0 c/deg) observations; there were not enough longitudinal data at 0.55 c/deg to include in this plot. Thresholds measured in the absence of masking noise show the expected pattern of change between infant and juvenile stages; thresholds in high masking noise are fairly constant at low spatial frequencies, but fall with age at the highest frequency.

available data to assign *all* additive factors to the periphery and *all* non-additive factors to central mechanisms, and to the degree that this assignment turns out to be incorrect our reasoning will need to be modified.

Our data do suggest that N_{eqC} and R_{sn} are to some degree independent and, therefore, that they measure different underlying processes. The best evidence for this is that the two parameters show quite different patterns of change with age at different spatial frequencies (Figs 6 and 8; Table 1), with N_{eqC} showing the most relative variation at low spatial frequencies and R_{sn} showing the most relative variation at the highest spatial frequency. At the lowest spatial frequency (0.55 c/deg), the changes in contrast threshold appear to be well-accounted for by changes in N_{eqC}, whereas at the highest spatial frequency, the changes in threshold are more strongly associated with changes in R_{sn}. If we consider the factors that relate most clearly to the changes in unmasked threshold, the simple correlations support the idea that R_{sn} is relatively more important at 4.2 c/deg than at other frequencies (see Table 1), while N_{eqC} has essentially uniform weight across spatial frequencies.

Our results at low spatial frequencies are consistent with those of Brown (1994), who measured the relative contribution of intrinsic noise to contrast discrimination thresholds in human infants and adults. Brown found a significant change in intrinsic noise between infants and adults using 0.55 c/deg grating stimuli, and a much smaller change in contrast-dependent, non-additive noise (Nc_1 in Brown, 1994), which is comparable with our factor R_{sn}. It is not known whether infant humans would show a similar shift in the influence of additive and non-additive factors at higher spatial frequencies as we found in the monkeys.

It follows from the logic spelled out above that one interpretation of this result is that peripheral changes account for the majority of sensitivity development at low spatial frequencies, while central changes have greater weight at higher frequencies. Recall that during development contrast thresholds fall more at higher spatial frequencies than at lower ones (Fig. 5; Boothe *et al.*, 1988). But inspection of Fig. 6 shows that N_{eqC} changes similarly at low and high spatial frequencies. It thus seems reasonable to suggest that in the absence of changes in central factors, sensitivity would improve uniformly at all spatial frequencies, and that the enhanced development of sensitivity at high spatial frequencies is due to changes in some central process.

What might the peripheral factor(s)limiting sensitivity be? Several candidate peripheral mechanisms have been proposed and analyzed previously (Banks & Bennett, 1988; Jacobs & Blakemore, 1988; Brown *et al.*, 1987; Brown, 1994; Allen, Bennett, & Banks, 1992; Wilson, 1993; Movshon & Kiorpes, 1993). Although such factors as growth of the eye and improvements in optical quality make modest contributions, the most important changes are likely to occur in the photoreceptors themselves, and in particular in the development of their outer segments into the efficient light-gathering devices seen in adults (Yuodelis & Hendrickson, 1986; Packer, Hendrickson, & Curcio, 1990). Such changes, like the changes in N_{eqC}, would have similar effects at all spatial frequencies within the limit of retinal sampling. Therefore, we tentatively suggest that the contribution of changes in N_{eqC} to the development of sensitivity depends on this early peripheral mechanism. In pursuit of this idea, we are presently developing an ideal observer model for the infant monkey, with which we expect to be able to analyze quantitatively the effects of factors like photoreceptor density and efficiency on ideal contrast sensitivity, and relate the results to our behavioral data.

What central mechanism(s) may be important for contrast sensitivity development is far from clear. One possibility is that the important "central" factor is in fact to be found at the level of the lateral geniculate nucleus. We and others have suggested that neurons at the level of

the LGN set an important limit on the normal development of acuity (Movshon & Kiorpes, 1993; Blakemore & Vital-Durand, 1986). However, recent electrophysiological measurements in the LGN of infant macaque monkeys suggest that there are relatively modest postnatal changes in spatial and temporal resolution, and that infant LGN neurons show a rather adult-like contrast response (Hawken, Blakemore, & Morely, 1997; Movshon, Kiorpes, Hawken, Skoczenski, Cavanaugh, & Graham, 1997). These and earlier studies do consistently show an overall improvement in neuronal responsiveness postnatally, a change which would be expected to have a similar effect across spatial frequencies.

Another possibility is simply that the central factors represent the strength and reliability of central synaptic connections in the visual system. There is ample anatomical and physiological evidence that these connections undergo extensive postnatal development in the visual cortex (see Daw, 1995). The changes in R_{sn} could simply reflect increases in synaptic gain or decreases in neuronal noise. But it is also possible that these effects are produced by changes in the spatial scale of the retinocortical projection produced by eye growth and photoreceptor migration (Packer *et al.*, 1990), or by changes in the fineness of spatial selectivity in spatial-frequency selective elements in visual cortex (Blakemore, 1990; Chino, Smith, Hatta, & Han, 1997). As a consequence of the refinement of receptive field structure that may underlie the development of high spatial-frequency selectivity, the elements sensitive to a given spatial frequency, say 4 c/deg, in infants may not be the same as in adults. For example, assuming that, as photoreceptors migrate and the fovea develops its adult photoreceptor density, the central connections formed early in development are maintained, the best spatial frequency for a given foveal V1 neuron will increase. The relatively different pattern of change we see in R_{sn} at the highest frequency may be reflecting such shifts. Ultimately, establishing which factors are the most important will require analysis of the physiological properties of neurons at several levels of the developing visual system, a project on which we have already embarked (Movshon, Hawken, Kiorpes, Skoczenski, Tang, & O'Keefe, 1994; Movshon *et al.*, 1997; Skoczenski, O'Keefe, Kiorpes, Tang, Hawken, & Movshon, 1995).

REFERENCES

Allen, D., Bennett, P. J. & Banks, M. S. (1992). The effects of luminance on FPL and VEP acuity in human infants. *Vision Research, 32*, 2005–2012.

Banks, M. S. & Bennett, P. J. (1988). Optical and photoreceptor immaturities limit the spatial and chromatic vision of human neonates. *Journal of the Optical Society of America A, 5*, 2059–2079.

Barlow, H. B. (1977). Retinal and central factors in human vision limited by noise. In Barlow, H. B. & Fatt, P. (Eds), *Vertebrate photoreception*. New York: Academic Press.

Baylor, D. A., Lamb, T. D. & Yau, K.-W. (1979). The membrane current of single rod outer segments. *Journal of Physiology, 288*, 589–611.

Blakemore, C. & Vital-Durand, F. (1986). Organization and postnatal development of the monkey's lateral geniculate nucleus. *Journal of Physiology, 380*, 453–491.

Blakemore, C. (1990) Maturation of mechanisms for efficient spatial vision. In Blakemore, C. (Ed.), *Vision: coding and efficiency*. Cambridge: Cambridge University Press.

Boothe, R. G., Kiorpes, L., Williams, R. A. & Teller, D. Y. (1988). Operant measurements of spatial contrast sensitivity in infant macaque monkeys during development. *Vision Research, 28*, 387–396.

Britten, K. H., Shadlen, M. N., Newsome, W. T. & Movshon, J. A. (1993). Responses of neurons in macaque MT to stochastic motion signals. *Visual Neuroscience, 10*, 1157–1169.

Brown, A. M. (1993). Intrinsic noise and infant visual performance. In Simons, K. (Ed.), *Early visual development: normal and abnormal*. New York: Oxford University Press.

Brown, A. M. (1994). Intrinsic contrast noise and infant visual contrast discrimination. *Vision Research, 34*, 1947–1964.

Brown, A. M., Dobson, V. & Maier, J. (1987). Visual acuity of human infants at scotopic, mesopic, and photopic luminances. *Vision Research, 27*, 1845–1858.

Burgess, A. E., Wagner, R. F., Jennings, R. J. & Barlow, H. B. (1981). Efficiency of human visual signal discrimination. *Science, 214*, 93–94.

Chino, Y. M., Smith, E. L., Hatta, S. & Han, C. (1997). Postnatal development of binocular disparity in neurons of the primate visual cortex. *Journal of Neuroscience, 17*, 296–307.

Croner, L. J., Purpura, K. & Kaplan, E. (1993). Response variability in retinal ganglion cells in primates. *Proceedings of the National Academy of Sciences USA, 90*, 8128–8130.

Daw, N. W. (1995). *Visual development*. New York: Plenum Press.

Finney, D. J. (1971). *Probit analysis*. New York: Cambridge University Press.

Gegenfurtner, K. R. & Kiper, D. C. (1992). Contrast detection in luminance and chromatic noise. *Journal of the Optical Society of America A, 9*, 1880–1888.

Handel, A., Kiorpes, L. & Movshon, J. A. (1993). Visual noise masking in a juvenile macaque. *Neuroscience Abstracts, 19*, 771.

Hawken, M.J., Blakemore, C. & Morely, J.W. (1997). Development of contrast sensitivity and temporal frequency selectivity in primate lateral geniculate nucleus. *Experimental Brain Research, 114*, 86–98.

Jacobs, D. S. & Blakemore, C. (1988). Factors limiting the postnatal development of visual acuity in the monkey. *Vision Research, 28*, 947–958.

Kersten, D. (1984). Spatial summation in visual noise. *Vision Research, 24*, 1977–1990.

Kiorpes, L. (1992). Development of vernier acuity and grating acuity in normally reared monkeys. *Visual Neuroscience, 9*, 243–251.

Kiorpes, L. & Kiper, D. C. (1996). Development of contrast sensitivity across the visual field in macaque monkeys (*Macaca nemestrina*). *Vision Research, 36*, 239–247.

Kiorpes, L., Kiper, D. C. & Movshon, J. A. (1993). Contrast sensitivity and vernier acuity in amblyopic monkeys. *Vision Research, 33*, 2301–2311.

Kiorpes, L., Skoczenski, A. M. & Movshon, J. A. (1995). Visual efficiency in young macaque monkeys. *Investigative Ophthalmology and Visual Science Suppl., 36*, 442.

Movshon, J. A., Hawken, M. J., Kiorpes, L., Skoczenski, A. M., Tang, C. & O'Keefe, L. P. (1994). Visual noise masking in macaque LGN neurons. *Investigative Ophthalmology and Visual Science Suppl., 35*, 1662.

Movshon, J. A. & Kiorpes, L. (1993). Biological limits on visual development in primates. In Simons, K. (Ed.), *Early visual development: normal and abnormal*. New York: Oxford University Press.

Movshon, J. A., Kiorpes, L., Hawken, M. J., Skoczenski, A. M., Cavanaugh, J. R. & Graham, N. V. (1997). Sensitivity of LGN neurons in infant macaque monkeys. *Investigative Ophthalmology and Visual Science Suppl., 38*, 498.

Packer, O., Hendrickson, A. E. & Curcio, C. A. (1990). Developmental redistribution of photoreceptors across the *Macaca nemestrina*

(Pigtail macaque) retina. *Journal of Comparative Neurology, 298*, 472–493.

Press, W. H., Teukolsky, S. A., Vetterling, W. T., & Flannery, B. P. (1992). *Numerical recipes in C.* (pp. 666–670). Cambridge: Cambridge University Press.

Pelli, D. G. (1981). Effects of visual noise. PhD Thesis. Cambridge University, Cambridge.

Pelli, D. G. (1990) The quantum efficiency of vision. In Blakemore, C. (Ed.), *Vision: coding and efficiency*. Cambridge: Cambridge University Press.

Shadlen, M. N. & Newsome, W. T. (1994). Noise, neural codes and cortical organization. *Current Opinion in Neurobiology, 4*, 569–579.

Skoczenski, A. M., O'Keefe, L. P., Kiorpes, L., Tang, C., Hawken, M. J. & Movshon, J. A. (1995). Visual efficiency of macaque LGN neurons. *Neuroscience Abstracts, 20*, 7.

Tolhurst, D. J., Movshon, J. A. & Dean, A. F. (1983). The statistical reliability of signals in single neurons in cat and monkey striate cortex. *Vision Research, 23*, 775–785.

Tolhurst, D. J., Movshon, J. A. & Thompson, I. D. (1981). The dependence of response amplitude and variance of cat visual cortical neurones on stimulus contrast. *Experimental Brain Research, 41*, 414–419.

Troy, J. B. & Lee, B. B. (1994). Steady discharges of macaque retinal ganglion cells. *Visual Neuroscience, 11*, 111–118.

Vogels, R., Spileers, W. & Orban, G.A. (1989). The response variability of striate cortical neurons in the behaving monkey. *Experimental Brain Research, 77*, 432–436.

Williams, R. A., Boothe, R. G., Kiorpes, L. & Teller, D. Y. (1981). Oblique effects in normally reared monkeys (*Macaca nemestrina*): meridional variations in contrast sensitivity measured with operant techniques. *Vision Research, 21*, 1253–1266.

Wilson, H. R. (1988). Development of spatiotemporal mechanisms in infant vision. *Vision Research, 28*, 611–628.

Wilson, H. R. (1993). Theories of infant visual development. In Simons, K. (Ed.), *Early visual development: normal and abnormal*. New York: Oxford University Press.

Yuodelis, C. & Hendrickson, A. E. (1986). A qualitative and quantitative analysis of the human fovea during development. *Vision Research, 26*, 847–855.

Acknowledgements—This research was supported by National Eye Institute grants EY05864 and EY02017, and PHS grant RR00166 to the Washington Regional Primate Research Center. We thank Martin Banks, Ari Handel, Ann Skoczenski, and Chao Tang for their contributions to this work, and Michael Hawken and Denis Pelli for comments on an early draft of this manuscript. We are indebted to Christine Brown, Jeanine Dimitri, Michael Gorman, and Jasmine Allen Siegel for assistance with animal care and testing.